

Variability of polymorphic families of three types of xylanase inhibitors in the wheat grain proteome

Non Peer-reviewed author version

Courtin, CM; CROES, Kristof; Gebruers, K.; ROBBEN, Johan; NOBEN, Jean-Paul; Samyn, B.; Debyser, G.; Van Beeumen, J. & Delcour, CM (2008) Variability of polymorphic families of three types of xylanase inhibitors in the wheat grain proteome. In: PROTEOMICS, 8(8). p. 1692-1705.

DOI: 10.1002/pmic.200700813

Handle: <http://hdl.handle.net/1942/8274>

1 **Variability of polymorphic families of three types of xylanase**
2 **inhibitors in the wheat grain proteome**

3
4 **Evi Croes¹, Kurt Gebruers¹, Johan Robben², Jean-Paul Noben²,**
5 **Bart Samyn³, Griet Debyser³, Jozef Van Beeumen³, Jan A. Delcour¹,**
6 **and Christophe M. Courtin¹**

7
8 ¹Laboratory of Food Chemistry and Biochemistry, Department of Microbial and Molecular systems,
9 Katholieke Universiteit Leuven, Kasteelpark Arenberg 20/2463, B-3001 Leuven, Belgium.

10 ²Biomedical Research Institute (BIOMED), Hasselt University and School of Life Sciences,
11 Transnationale Universiteit Limburg, Campus Diepenbeek, B-3590 Diepenbeek, Belgium.

12 ³Laboratory for Protein Biochemistry and Protein Engineering, Universiteit Gent, K.L. Ledeganckstraat
13 35, B-9000 Gent, Belgium.

14
15 **Corresponding author:** Evi Croes, Laboratory of Food Chemistry and Biochemistry,
16 Katholieke Universiteit Leuven, Kasteelpark Arenberg 20/2463, B-3001 Leuven,
17 Belgium.

18 Tel.: + 32 16321634. Fax: + 32 16321997.

19 E-mail address: evi.croes@biw.kuleuven.be.

20
21 **Abbreviations used:** AC, affinity chromatography; CEC, cation exchange
22 chromatography; CNBr, cyanogen bromide; GH, glycoside hydrolase; λ PPase,
23 lambda protein phosphatase; PAA, polyacrylamide; PABs, polyclonal antibodies;
24 TAXI, *Triticum aestivum* xylanase inhibitor; TFMS, trifluoromethanesulfonic acid;
25 TLXI, thaumatin-like xylanase inhibitor; XI, xylanase inhibitor; XIP, xylanase
26 inhibiting protein

27
28 **Keywords:** polymorphism/wheat/xylanase inhibitors

29 **ABSTRACT**

30 Cereals contain proteinaceous inhibitors of endo- β -1,4-xylanases (E.C.3.2.1.8,
31 xylanases). Since these xylanase inhibitors (XIs) are only active against xylanases of
32 microbial origin and do not interact with plant endogenous xylanases, they are
33 believed to act as a defensive barrier against phytopathogenic attack. So far, three
34 types of XIs have been identified, i.e. *Triticum aestivum* XI (TAXI), xylanase
35 inhibiting protein (XIP), and thaumatin-like XI (TLXI) proteins. In this study the
36 variation in XI forms present in wheat grain was elucidated using high-resolution 2-
37 DE in combination with LC-ESI-MS/MS and biochemical techniques. Reproducible
38 2-DE fingerprints of TAXI-, XIP-, and TLXI-type XIs, selectively purified from
39 whole meal of three European wheat cultivars using cation exchange chromatography
40 (CEC) followed by affinity chromatography (AC), were obtained using a pH-gradient
41 of 6 to 11 and a molecular mass range of 10 to 60 kDa. Large polymorphic XI
42 families, not known to date, which exhibit different *pI*- and/or molecular mass values,
43 were visualised by colloidal CBB staining. Identification of distinct genetic variants
44 by MS/MS-analysis provides a partial explanation for the observed XI heterogeneity.
45 Besides genetic diversity, PTMs, such as glycosylation, account for the additional
46 complexity of the 2-DE patterns.

47 **1 INTRODUCTION**

48 Endo- β -1,4-xylanases (E.C.3.2.1.8, further referred to as xylanases) are crucial
49 enzymes in the breakdown of arabinoxylan, the predominant cell wall non-starch
50 polysaccharide of cereals like wheat [1]. Most of the xylanases are confined to
51 glycoside hydrolase (GH) families 10 and 11 [2].

52 Little is known about plant endogenous xylanases, which are believed to play a role in
53 cell wall metabolism, seed germination and pollination [3]. In contrast, a large
54 number of microbial xylanases has been described. Micro-organisms synthesize these
55 xylanases, next to other cell wall-degrading enzymes, to provide assimilable nutrients
56 for development. Moreover, xylanases from phytopathogenic species are important
57 virulence factors as they facilitate disintegration of plant cell walls at the host
58 penetration site [4-7]. Several microbial xylanases have been adopted by the paper
59 and pulp industry to reduce the need for chemical bleaching [8] and by the cereal-
60 based food and feed industries to improve processing and/or product quality [9-12].

61 One of the strategies of plants to try to impede invasion by microbial pathogens is by
62 producing antimicrobial agents [13] such as specific enzyme-inhibiting proteins.
63 These can counteract the action of microbial cell wall-degrading enzymes and hence
64 limit colonisation, as was demonstrated for polygalacturonase inhibitors present in
65 several dicotyledonous plants [14].

66 In wheat, three types of xylanase inhibitor proteins (XIs) have been discovered over
67 the last decade, *i.e.* *Triticum aestivum* XI (TAXI) [15], xylanase inhibitor protein
68 (XIP) [16], and thaumatin-like XI (TLXI) [17] which, in view of their specificity for
69 microbial xylanases, and, in the case of TAXI and XIP, their demonstrated
70 inducibility by pathogens [18, 19], most likely classify as plant defence-related
71 proteins.

72 TAXI-type XIs are a mixture of high-*pI* inhibitors, TAXI-I to TAXI-IV, with distinct
73 specificities towards xylanases [18, 20]. They occur simultaneously as a ~40 kDa
74 single polypeptide and as a processed form existing of two disulfide-linked
75 polypeptides of ~30 and ~10 kDa [20]. XIP- and TLXI-type XIs are basic, monomeric
76 proteins with a molecular mass of ~30 and ~18 kDa, respectively [16, 17]. Multiple
77 putative TAXI- [18, 21, 22] and XIP-type [19, 23] as well as one TLXI-type gene(s)
78 [17] have been identified in wheat and some have been confirmed. For the three types
79 of XIs, the existence of various forms as well as differences in their spatio-temporal
80 location, due to distinct regulatory control mechanisms, have been suggested. Igawa
81 and co-workers [18, 19] demonstrated that *Taxi-III* and *-IV* transcripts mostly
82 accumulate in roots and older leaves, in contrast to *Taxi-I*. Furthermore they found
83 that expression of *Taxi-III* and *Taxi-IV*, in addition to that of *Xip-I*, is pathogen-
84 inducible. Based on these observations it is speculated that, in analogy with
85 polygalacturonase inhibitors [24], large families of isoforms have adaptively co-
86 evolved with antagonistically active microbial xylanases to achieve a superior
87 counterattack against pathogens. In contrast, *Taxi-I* transcripts are not induced by
88 infection, suggesting a distinct physiological role *in planta* [18]. Together, the three
89 types of XIs make up a significant proportion (approx. 2.5%) of the physiologically
90 active albumin/globulin population, present in wheat grain. Thus, it is logical to
91 assume that this group of proteins can be of great meaning for the wheat plant. Their
92 importance in reducing the activity of added microbial xylanases in wheat-based food
93 processes has already convincingly been demonstrated [25-28] and led to the
94 development of inhibitor-insensitive xylanases, less prone to year-to-year wheat
95 inhibitor content variations [29-31].

96 Despite extensive characterization of TAXI-, XIP-, and TLXI-type XIs, there is a lack
97 of knowledge on their polymorphism in wheat grain. The aim of this study was to
98 elucidate this unknown heterogeneity using high-resolution 2-DE and subsequent MS
99 analysis. For the first time a study was undertaken concurrently for the three types of
100 wheat XIs.

101 **2 MATERIALS AND METHODS**

102 **2.1 Materials**

103 Wheat cultivars Claire (harvest 2005), Zohra and Koch (harvest 2003) were obtained
104 from AVEVE (Landen, Belgium) and ground into whole meal using a Cyclotec 1093
105 sample mill (Tecator, Hogånäs, Sweden). Grindamyl H640 bakery enzyme,
106 containing a *Bacillus subtilis* GH family 11 xylanase, was purchased from Danisco
107 (Braband, Denmark). *Penicillium purpurogenum* GH family 10 xylanase was kindly
108 made available by Prof. Jaime Eyzaguirre (Laboratorio de Bioquímica, Facultad de
109 Ciencias Biológicas, Pontificia Universidad Católica de Chile, Chile). A GH family
110 11 xylanase from *Aspergillus niger* and Xylazyme AX tablets, which comprise
111 azurine cross-linked wheat arabinoxylan, were from Megazyme (Bray, Ireland). All
112 other reagents, BSA, casein, synthetic peptides and bacteriophage λ protein
113 phosphatase (λ PPase) were purchased from Sigma-Aldrich (Bornem, Belgium).

114

115 **2.2 Extraction of wheat soluble seed proteins**

116 Wheat whole meal was ground in liquid nitrogen using mortar and pestle, and 250 mg
117 fine powder was suspended in 1.0 ml ice-cold extraction buffer [50 mM Tris-HCl pH
118 7.8, Complete Protease Inhibitor Cocktail (1 tablet/10 ml buffer, Roche Diagnostics,
119 Vilvoorde, Belgium)], incubated for 10 min on ice with intermittent mixing and
120 centrifuged (14000g; 15 min, 4°C). Proteins were precipitated (overnight, -20°C) by
121 addition of 4 volumes 10% TCA in acetone. Pellets were washed twice with 80%
122 acetone and air-dried.

123

124 **2.3 Purification of xylanase inhibitors from wheat whole meal**

125 Purification of the three types of XIs in wheat whole meal was performed using cation
126 exchange chromatography (CEC) followed by affinity chromatography (AC) with
127 immobilised xylanases according to a protocol described by Gebruers *et al.* [32] with
128 a few modifications. The procedure was down-scaled and extended storage times,
129 during which the protein population may undergo unwanted modifications, e.g. due to
130 wheat endogenous enzymes, were avoided. TAXI-type proteins were bound to the
131 first AC column, coupled with a GH family 11 *B. subtilis* xylanase. Isolation of XIP-
132 and TLXI-type proteins was performed in a second affinity-based step, this time with
133 an immobilized GH family 11 *A. niger* xylanase as biospecific ligand. Protein
134 concentrations were estimated according to Bradford [33] with BSA as standard.

135 A second, modified procedure for purification of XIs from wheat whole meal was
136 performed to affirm or disaffirm the generation of artefacts during extraction and
137 isolation. Complete Protease Inhibitor Cocktail (1 tablet/ 50 ml buffer) and pepstatin
138 A (35 µg/ 50 ml buffer) were added to the aqueous extraction solution as well as to
139 the eluates of the CEC column. Furthermore, all extraction and purification steps were
140 performed at 7°C and in the shortest time period possible (~3 days).

141

142 **2.4 2-DE and staining**

143 TCA-acetone pellets of crude wheat soluble proteins (see above) were dissolved in
144 150 µl lysis buffer (7.0 M urea, 2.0 M thiourea, 4.0% CHAPS, 20 mM DTT, 0.5%
145 IPG pH 6-11 buffer, trace of bromophenol blue) and the protein concentration was
146 measured using the 2D-Quant-kit (GE Healthcare, Uppsala, Sweden) as described by
147 the manufacturer. Affinity-purified XI fractions (see above) were desalted and
148 concentrated to ca. 2.0 mg/ml by means of ultrafiltration using Vivaspin 15R
149 concentrators with a molecular mass cut-off of 5,000 Da (Sartorius AG, Goettingen,

150 Germany). Forty microgram protein aliquots were fully denatured by addition of lysis
151 buffer.

152 Immobiline Drystrips pH 6-11 (18×0.3×0.5 cm) were reswollen overnight in 340 µl
153 Destreak rehydration solution (GE Healthcare) containing 0.5% IPG buffer. Samples
154 were cup-loaded near the anode and focused at 20°C using the Ettan IPGphor II IEF
155 unit (GE Healthcare). The running parameters for IEF were 500 V (120 min), 500-
156 1000 V (60 min), 1000-10000 V (180 min), and 10000 V (55 min), reaching a total of
157 at least 27 kVh. Prior to SDS-PAGE, the IPG-strips were reduced for 15 min at room
158 temperature (RT) using an equilibration buffer (6.0 M urea, 50 mM Tris-HCl pH 8.8,
159 2% SDS, 30% glycerol, trace of bromophenol blue) containing 65 mM DTT, followed
160 by an alkylation step of 15 min at RT with the same buffer containing 135 mM
161 iodoacetamide. The IPG strips were then transferred to 15% homogenous
162 polyacrylamide (PAA) gels (25×20×0.1 cm) and SDS-PAGE was performed at 20°C
163 using the Ettan Daltsix vertical electrophoresis system in conjunction with the Tris-
164 glycine buffer system [34]. Protein entry was accomplished at 2 W/gel for 45 min,
165 followed by separation at 17 W/gel for 4.5 h. 2-DE gels were stained with the
166 sensitive CBB G-250 method as described by Candiano *et al.* [35] or using silver
167 staining based on Blum *et al.* [36] and scanned via the ImageScanner II system with
168 accompanying Labscan 5.00 software (GE Healthcare).

169 To selectively visualise the glycoproteins present in 2-DE gels a sequential
170 fluorescence-based staining procedure, comprising the Pro-Q® Emerald 300
171 Glycoprotein stain and the Sypro Ruby total protein stain (Invitrogen, Carlsbad, CA,
172 USA) was applied according to the manufacturer's instructions.

173

174 **2.5 Protein identification by tandem mass spectrometric analysis**

175 Protein spots were picked manually from CBB stained gels, and trypsin-digested
176 according to the method of Shevchenko *et al.* [37]. Tryptic digests were analyzed by
177 LC-ESI-MS/MS on a LCQ Classic (Thermo Electron, San Jose, CA, USA) ion trap
178 MS equipped with a nano-LC column switching system as described by Dumont *et al.*
179 [38]. MS/MS data were searched against the Viridiplantae division of the GenBank
180 non-redundant protein database using the Mascot (Matrix Sciences, London, U.K.)
181 and against a custom database using the Sequest (Thermo Electron) algorithm. The
182 latter contained all GenBank plant XI sequences as of 10 October 2007, as well as
183 clustered XI-encoding EST sequences. In addition, recently submitted putative TAXI
184 sequences were added to the custom database. The SEQUEST/MASCOT mass
185 tolerance for parent and fragment ions were +3 and +1 Da, respectively.
186 Carbamidomethylation of Cys and oxidation of Met, Trp and His were set as fixed
187 and variable modifications, respectively. Maximally one missed cleavage was
188 allowed, and the neutral loss of water and ammonia from b- and y-ions was taken into
189 consideration. To allow detection of eventually truncated N- and C-termini, the
190 custom database was subsequently N- and C-terminally ‘ragged’ using DBToolkit
191 version 3.1 [39]. For every ‘parent’ sequence the ‘ragging’ process created a series of
192 subsequences. From each n -th subsequence (with $1 \leq n \leq 30$), the first $n-1$ residues
193 were removed from the N- and C-termini.

194

195 **2.6 C-terminal and *de novo* sequence analysis**

196 Cyanogen bromide (CNBr)-fragments were generated for C-terminal analysis [40].
197 *De novo* sequence analysis of chemically derivatized peptides was carried out
198 essentially as described previously [41]. Mass analysis was performed on an Applied
199 Biosystems 4700 Proteomics Analyzer with TOF/TOF optics [42]. Samples were

200 prepared by spotting 1 μ l of a mixture of sample and matrix (7 mg/ml CHCA in 50%
201 ACN containing 0.1% TFA) on a stainless steel (192-well) MALDI target plate and
202 allowed to air-dry at RT. Prior to MALDI-MS analysis, the instrument was externally
203 calibrated with a mixture of Angiotensin I, Glu-fibrino-peptide B, ACTH (1-17), and
204 ACTH (18-39). For MS/MS experiments, the instrument was externally calibrated
205 with fragments of Glu-fibrino-peptide.

206

207 **2.7 Immunoblot analysis**

208 Polyclonal antibodies (PABs), specifically interacting with TAXI-, XIP- or TLXI-type
209 XIs, were obtained by rabbit immunisation as described by Beaugrand and co-workers
210 [43]. Further purification of the PABs by AC with immobilised native TAXI-, XIP- or
211 rTAXI-type inhibitors improved specificity. 2-DE separated proteins were
212 electroblotted (16V, 40 min) onto an activated Protran (0.45 μ m pore size)
213 nitrocellulose membrane (Schleicher and Schuell, Dassel, Germany) and probed with
214 anti-TAXI, anti-XIP and anti-TLXI PABs as described before [43].

215

216 **2.8 Determination of apparent xylanase inhibitor activity**

217 Apparent XI activities of wheat whole meal fractions or run-through fractions of CEC
218 and AC columns were determined colorimetrically with the Xylazyme AX method as
219 described by Gebruers *et al.* [20]. Conversion of XI activities into inhibitor levels was
220 described by Dornez *et al.* [44]. The levels of TAXI- and XIP-type inhibitors were
221 measured using a specific GH family 11 *B. subtilis* xylanase and a GH family 10 *P.*
222 *purpurogenum* xylanase, respectively.

223

224 **2.9 Chemical deglycosylation of xylanase inhibitors**

225 Affinity-purified and desalted XIs were lyophilized in small glass vials to create a
226 moisture-free atmosphere for deglycosylation with trifluoromethanesulfonic acid
227 (TFMS) [17, 45]. Briefly, dry sample aliquots (500 µg) were incubated (180 min) on
228 ice with a pre-cooled 10.0% anisole in TFMS solution and neutralized by gradually
229 adding droplets of a 60% pyridine solution, thereby keeping the samples at -15°C in a
230 MeOH/dry ice bath. Prior to 2-DE, pellets were dissolved in lysis buffer (see above).

231

232 **2.10 Enzymatic dephosphorylation of xylanase inhibitors**

233 Affinity-purified and desalted XIs were dephosphorylated using broad spectrum λ-
234 PPase. Forty microgram protein aliquots were prepared in 50 µl λ-PPase buffer (50
235 mM Tris-HCl pH 7.8, 5.0 mM DTT) and incubated for 24 h at 30°C with 0 (negative
236 control sample) and 800 units of enzyme in the presence of 2.0 mM MnCl₂.
237 Ovalbumin (GE Healthcare) and casein were treated in a similar way and used as
238 positive control samples, while BSA was used as a negative control. After
239 dephosphorylation, proteins were desalted and concentrated by means of ultrafiltration
240 using Microcon YM-3 centrifugal filter units with molecular mass cut-off of 3,000 Da
241 (Millipore, Billerica, MA, USA). Prior to SDS-PAGE and 2-DE analysis, proteins
242 were dissolved in sample buffer (see below) and lysis buffer (see above), respectively.

243

244 **2.11 1-D gel electrophoresis and staining**

245 SDS-PAGE was performed on commercial 20% PAA gels using the PhastSystem unit
246 (GE Healthcare). Proteins were denatured in sample buffer (10% glycerol, 62.5 mM
247 Tris-HCl pH 6.8, 2% SDS (w/v), 5% 2-mercaptoethanol (v/v), trace of bromophenol
248 blue). For serial detection of phosphoprotein and total protein profiles, Pro-Q®
249 Diamond Phosphoprotein gel staining (Invitrogen) and subsequent silver staining were

250 performed according to the manufacturer's instructions. Phosphoproteins were
251 visualised with a Typhoon 9400 laser fluorescence scanner (GE Healthcare) at an
252 excitation wavelength of 532 nm and using a 560 nm long pass emission filter.

253 **3 RESULTS AND DISCUSSION**

254 **3.1 2-DE of wheat soluble seed proteins**

255 Since all three types of XIs are high-*pI* proteins [46], high-resolution separation of
256 wheat seed proteins (cultivar Claire, Fig. 1) was realized in a linear alkaline pH-
257 gradient of 6 to 11. SDS-PAGE was achieved on 15% homogenous PAA gels,
258 covering a molecular mass range between 10 and 60 kDa, ideally suited for the
259 separation of the three classes of XIs.

260 Evaluation of the 2-DE pattern (Image Master 2D-Platinum software, GE Healthcare)
261 resulted in the detection of over a thousand spots. To reveal the presence and location
262 of the three classes of XIs in this complex pattern of wheat seed proteins, 2D-gels
263 were subjected to immunoblotting with PABs, specifically reacting with TAXI-, XIP-
264 or TLXI-type XIs. Fig. 1 shows that the extraction/precipitation procedure and
265 subsequent 2-DE analysis preserved the three classes of XIs, as immunostaining was
266 observed for the 40 and 30 kDa polypeptides of TAXI-type proteins, as well as for
267 XIP- and TLXI-type XIs. As expected, the 10 kDa C-terminal parts of the cleaved
268 form of TAXI-type proteins escaped this pH-range, given their more acidic *pI*-values
269 (*pI* 5.0-5.3) [20].

270 The large number of spots, detected with western blotting and probing with XI-
271 specific PABs, was not anticipated. To reveal the large heterogeneity in XIs and, in
272 addition to allow detection and identification of relatively low-abundant forms, a
273 selective enrichment of the target proteins was performed.

274

275 **3.2 2-DE of isolated polymorphic wheat xylanase inhibitors**

276 **3.2.1 Purification of the three types of wheat xylanase inhibitors**

277 To reduce the large number of non-inhibitor proteins present in wheat grain extracts
278 while retaining all different forms of the three classes of XI-proteins, a selective,
279 chromatographic pre-fractionation step was performed.
280 TAXI-, XIP- and TLXI-type XIs were isolated from wheat whole meal extracts
281 originating from three European wheat cultivars, selected for their distinct XI
282 activities. TAXI and XIP levels, measured *in vitro* by the Xylazyme AX method, were
283 110, 90 and 155 ppm, and 375, 300 and 325 ppm, for the Claire, Koch and Zohra
284 cultivars, respectively. Following extraction and concentration by CEC, wheat whole
285 meal extracts were applied on a series of two affinity columns. Only members of the
286 TAXI inhibitor class were retained by the *B. subtilis* xylanase, while the *A. niger*
287 xylanase bound the remaining two types of inhibitors.

288

289 **3.2.2 2-DE fingerprints of purified xylanase inhibitors**

290 For affinity-purified, desalted protein fractions, containing almost solely TAXI-type
291 (Fig. 2A) or XIP-/TLXI-type (Fig. 3A) XIs, reproducible high-resolution spot
292 fingerprints were obtained in the pH-gradient 6-11, and with SDS-PAGE on 15%
293 PAA gels. Thus, TAXI-, XIP- as well as TLXI-type inhibitors exhibit a large
294 variability in molecular mass and/or *pI* within a single wheat cultivar, as was expected
295 from the western blot experiment. Moreover, despite some small differences between
296 these 2-DE fingerprints (Figs. 2A and 3A) and the immunoblotted 2-DE patterns (Fig.
297 1), possibly due to differences in inhibitor concentration or presence/absence of other
298 wheat seed proteins, the overall spot patterns were very similar, validating the
299 affinity-based purification.

300 For the spots identified as TAXI-type proteins (see paragraph 3.3.1), only small
301 differences in molecular mass could be detected, while a large variation in *pI*-values

302 was visible (Fig. 2A). Estimated molecular masses were 45-46 kDa for the non-
303 cleaved form and 32-33 kDa for the N-terminal polypeptides of processed TAXI-type
304 proteins. These values are slightly higher than expected from their amino acid
305 sequences. A few faint spots with lower molecular masses (41-44 kDa and 25-27
306 kDa), were observed as well. They may have arisen from partial break-down of the
307 TAXI protein, albeit without major structural changes to the active site as they still
308 bind to the enzymes on the affinity columns. The non-processed form of TAXI-type
309 proteins corresponded to spots with *pI*-values between ~7.5 and ~9.5, while the *pI*-
310 range for the N-terminal polypeptides of the processed form varied between ~8.9 and
311 9.5. In contrast to TAXI-type inhibitors, the spots, identified as XIP-type proteins (see
312 paragraph 3.3.1), showed much greater variability in molecular mass (Fig. 3A). The
313 2-DE pattern consisted of vertical rows of spots with molecular masses varying
314 between 29 and 36 kDa, which were positioned at *pI*-values between ~7.2 and ~9.4.
315 The same was true for the spots identified as TLXI proteins (see paragraph 3.3.1),
316 except that there was only one row of spots at *pI* ~9.8 and within a molecular mass
317 range of 18-21 kDa. As for TAXI-type inhibitors, a few weak spots of XIP-(iso)forms
318 were visible at lower molecular masses.

319 Furthermore, the 2-DE patterns obtained for the polymorphic families of XIs, present
320 in cultivar Claire, were very similar for the cultivars Koch (Figs. 2B and 3B) and
321 Zohra (Figs. 2C and 3C). About 95% of all XI forms (matched in Image Master 2D-
322 Platinum software) were found in the three cultivars. Spots 45-47 (Fig. 3A) from
323 cultivar Claire were slightly shifted in cultivars Koch and Zohra, possibly because of
324 variable post-translational modifications or (homoeo)allelic variation and, more
325 exceptionally, the cultivar Zohra did not show spots near 18-21 kDa, which implies

326 that TLXI-type proteins are not present, or only present in undetectable amounts in
327 this cultivar.

328

329 **3.3 Identification of affinity-purified proteins**

330 **3.3.1 Xylanase inhibitor proteins**

331 Using LC-ESI-MS/MS most of the protein spots (Figs. 2A and 3A) were identified as
332 XIs (Table 1, Supplementary Table 1). Moreover, an attempt was undertaken to
333 distinguish between genetic variants, despite their limited differences in amino acid
334 sequences.

335 Until recently, gene sequences of six TAXI variants have been published, i.e. *Taxi-Ia*
336 (AJ438880) [21], *Taxi-Ib* (AJ697851), *Taxi-IIa* (AJ697849), *Taxi-IIb* (AJ697850)
337 [22], *Taxi-III* (AB178471) and *Taxi-IV* (AB114628) [18]. In addition, six putative
338 wheat TAXI-sequences, *Taxi-725ACCN* (EU082811), *Taxi-725ACC* (EU082810),
339 *Taxi-725OS* (EU082812), *Taxi-602OS* (EU082813) *Taxi-801OS* (EU082814) and
340 *Taxi-801NEW* (EU082815) were made available too.

341 In total, 24 spots were unequivocally (from 3 up to 20 non-redundant significant
342 peptide hits per spot) identified as TAXI-type proteins (Table 1, Supplementary Table
343 2). Among these, 13 spots correspond to full-length TAXI form A (Fig. 2A, spots 1-
344 13), and 11 spots to the 30 kDa fragment of form B (Fig. 2A, spots 14-24). The
345 conserved cleavage site separating the 30 and 10 kDa TAXI polypeptides is indicated
346 in Fig. 4. The high amino acid sequence similarity among the TAXI variants and
347 hence the limited amount of variant specific tryptic peptides (Fig. 4), however, often
348 confounded the search engines Mascot and Sequest, thereby complicating the proper
349 assignment of spectra to a specific TAXI variant. Therefore, TAXI variants were
350 tentatively assigned by manually calculating the maximum number of significantly

351 scored, variant matching peptide hits in each spot. When not all peptides could be
352 matched to a single variant, a second or third tentative assignment of the spectra to
353 other TAXI variants was performed. In this way, all 847 significantly scored tandem
354 MS spectra could be ascribed to minimally 4 out of 12 TAXI sequence variants,
355 present in our customized database, being TAXI-Ia, TAXI-IIa, TAXI-IV and TAXI-
356 725ACCN. The occurrence of the variant TAXI-IIb (one specific peptide hit) cannot
357 be excluded because only a two amino acid difference exists between TAXI-IIb and
358 TAXI-IV, resulting in just two detectable distinct tryptic peptides. The same is true
359 for TAXI-725ACCN and TAXI-725ACC, for which eight differences in amino acids
360 exist, giving rise to only five detectable distinct tryptic peptides. None of the TAXI-
361 725ACC specific peptides was observed, however. They could all be accounted for as
362 originating from TAXI-725ACCN. Tryptic peptides specific for TAXI-Ib or TAXI-
363 III, which show 99.6% identity, were not found in the corresponding 2-DE spot
364 patterns. To date, TAXI-Ib has only been produced recombinantly in *Pichia pastoris*
365 [22], while *Taxi-III* transcripts were only demonstrated to occur in lemma, palea and
366 leaves of the wheat plant after pathogen inoculation [18]. It should be noted that the
367 presence of other highly similar TAXI sequence variants cannot be ruled out either.
368 After all, our data show that single spots often contain different TAXI sequence
369 variants, and that each TAXI variant occurs in several different spots (Table 1).
370 Regarding the identification of XIP-type proteins, the situation was less complex
371 (Table 1). Full-length gene sequences were already described for *Xip-I* (Q8L5C6) [23]
372 and *Xip-III* (BAD99103) [19]. Most recently Takahashi-Ando and co-workers [47]
373 revealed the existence of *Xip-R1* (BAF74363) and *Xip-R2* (BAF74364) genes. In our
374 analyses, the presence of both XIP-I (Fig. 3A, spots 30, 32-51) and XIP-III (Fig. 3A,
375 spots 25-29, 31) in the 2-DE pattern was confirmed, while none of the MS/MS spectra

376 could be matched to XIP-R1 or XIP-R2. The latter two XIP-type family members
377 probably reside in wheat plant parts, other than the caryopsis, or occur under other
378 (stress) conditions. In total, 27 spots were unequivocally determined as XIP proteins
379 (Supplementary Table 3). For the third class of XIs, all observed spots (Fig. 3A, spots
380 52-55) correspond to the only TLXI encoding gene sequence (Table 1) thus far
381 identified in wheat [17].

382 Most of the XI forms migrated to positions in the 2-DE gel which were in agreement
383 with their theoretical pI -values, e.g. TAXI-725ACCN and XIP-III forms, which have
384 the lowest theoretical pI -values among the XI proteins, were situated close to the
385 neutral part of the pH-range.

386 Most prominent in the identification of different genetic variants was the observation
387 that the number of protein spots in the 2-DE patterns of all three classes of XIs highly
388 exceeded the number of distinguished genetic variants. To check the possibility that
389 the large variation was caused by proteolytic activity or other side reactions during the
390 protein isolation, the extraction/purification of the three classes the XIs was carried
391 out again for the cultivar Claire. This time a mixture of protease inhibitors was added
392 and the temperature was reduced to prevent the formation of artificial products as
393 much as possible. Comparison of the 2-DE fingerprints, acquired for the multiple
394 (iso)forms of the three classes of XIs, didn't reveal differences between the outcomes
395 of the standard and the modified purification procedure (results not shown), implying
396 that no artefacts were produced either due to endogenous proteolytic activity or
397 enzymatic side reactions. Hence, the large heterogeneity in inhibitor forms is most
398 likely caused *in planta* by PTMs. It can not be excluded, however, that other XI gene
399 sequences exist, which are thus far unknown because of the size and complexity of
400 the hexaploid, not yet fully sequenced, wheat genome.

401 XIs in wheat grains thus are present as multiple forms, displaying charge- and
402 molecular mass heterogeneity and, at least TAXI- and XIP-type XIs seem to be
403 organized in multigene families. These observations fit well with their suggested role
404 as plant defence-related proteins and are in line with observations on
405 polygalacturonase inhibitors, which evolved as large families with specific
406 recognition abilities against the many polygalacturonases produced by
407 phytopathogenic fungi [24]. Thus far, different xylanase specificities of TAXI-I- and
408 TAXI-II-type XIs have been demonstrated [20]. It is thus not unlikely that XIs too
409 underwent a co-evolution with their pathogenic counterparts, resulting in the presence
410 of a large heterogeneity in expressed forms, conferring enhanced resistance to
411 multiple pathogens [48]. Igawa and co-workers [18] provided evidence for induced
412 expression of *Taxi-III* and *Taxi-IV* in lemma/palea or leaves upon infection with *F.*
413 *graminearum* and *E. graminis*, while expression of *Taxi-I* is only up-regulated in
414 response to abiotic stress. Furthermore it has been demonstrated that *Xip-I* and *Xip-*
415 *R1*, but not *Xip-III* and *Xip-R2*, are strongly transcribed in infected wheat leaves,
416 though this appears to be pathogen-dependent [19, 47]. Wounding, as well as
417 treatment of leaves with methyl jasmonate, also enhance the expression of *Xip-I* [19].
418 Accordingly, it is hypothesized that, within the large polymorphism, some XI forms
419 are basal pre-existing defence-related proteins, while others have a more specialized
420 protective role triggered by specific biotic or abiotic stimuli [19, 47].

421

422 **3.3.2 Non-xylanase inhibitor proteins**

423 From Fig. 2A it can be deduced that, next to spots corresponding to TAXI-type
424 inhibitors, the XI protein preparation also contained some impurities, co-purified on
425 the *B. subtilis* affinity matrix (Supplementary Table 1). Among these, a bifunctional

426 α -amylase inhibitor, a class II chitinase, LMW glutenin subunits, a thaumatin-like
427 protein TLP7, β -glucosidases and some unidentified proteins were coupled, probably
428 by non-specific interactions. In the area near neutral *pI* (6.0-7.0) and low molecular
429 mass (< 18 kDa), a small group of intense spots could be matched by MS/MS to α -
430 amylase inhibitors (Table 1). Their high abundance in the purified XI fraction was
431 surprising. In contrast to other impurities present, the pattern of the α -amylase
432 inhibitors remained unaltered, irrespective of purification scheme or wheat cultivar
433 (Fig. 2). It is not yet clear whether these proteins interact with the *B. subtilis* xylanase
434 or with TAXI-type inhibitors, and whether they possess any XI activity in addition to
435 their α -amylase inhibitor activity.

436

437 **3.4 Post-translational modifications**

438 The high multiplicity of spots, identified as the same gene product but differing in
439 molecular mass and/or *pI*, supports the occurrence of different PTMs for the three
440 types of XIs, independent of wheat cultivar. In order to gain more insight into the
441 post-translational heterogeneity of the polymorphic families of wheat XIs, some of
442 the most commonly occurring PTMs were examined.

443

444 **3.4.1 Spots with a different molecular mass and the same *pI***

445 XIP- and TLXI-type XIs show vertical rows of spots in their 2-DE patterns, indicative
446 for varying degrees of glycosylation, whereas less variation in molecular mass is seen
447 for TAXI-type proteins. TAXI-type XIs have a predicted N-glycosylation site at
448 Asn¹⁰⁵ (TAXI-Ia and TAXI-725ACCN) or Asn¹⁰⁷ (TAXI-IV/IIb and TAXI-IIa) (Fig.
449 4) [48]. XIP-I/XIP-III and TLXI have a Asn-X-Ser/Thr motif at positions 89 and 95,
450 respectively [17, 49].

451 To reveal the non-glycosylated ‘parent’ 2-DE pattern for the three types of XIs,
452 chemical deglycosylation of the affinity-purified proteins was accomplished using
453 TFMS. As expected for XIP- and TLXI-type proteins (Fig. 5B), the vertical trains of
454 spots disappeared due to the acid treatment. For TAXI-type proteins (Fig. 5A) no
455 differences in molecular mass were seen, however, a noticeable shift in *pI* was
456 observed upon deglycosylation. This was even more so the case for XIP- and TLXI-
457 type proteins. One reason for this shift towards the cathode upon deglycosylation may
458 be the removal of negatively charged sialic acid residues which are possibly build-in
459 as part of the complex carbohydrate structure [51]. A pathway for sialylation was only
460 recently discovered in plants [50] and, moreover, for TLXI, the incorporation of one
461 sialic acid residue in the glycan structure has been described [17]. Although it can not
462 be taken for granted, it has been demonstrated that the effect of TFMS, in the
463 presence of anisole as scavenger, is sufficiently specific, in the sense that the protein
464 backbone and the PTMs, other than glycosylation are stable during the treatment [45,
465 52].

466 To complement the above results, TAXI- and XIP-/TLXI-type proteins were, before
467 and after deglycosylation, stained with the fluorescent Pro-Q Emerald 300
468 glycoprotein stain. The small signal for TAXI-type proteins (Fig. 6A) disappeared
469 upon deglycosylation, while the intense glycoprotein signal of XIP- and TLXI-type
470 inhibitors (Fig. 6B) remained only slightly visible (result not shown). The residual
471 fluorescence may have been due to the presence of N-acetylhexosamine of N-linked
472 glycans that escapes removal by TFMS [45]. Post-staining with Sypro Ruby
473 confirmed the presence of XI spots in gels giving no Pro-Q Emerald signal.

474

475 **3.4.2 Spots with a different *pI* and the same molecular mass**

476 In the case of TAXI- (Fig. 2) and XIP-type (Fig. 3) inhibitors, all genetic variants,
477 identified by MS, emerge as multiple spots with distinct *pI*-values. Conversely, TLXI-
478 type (Fig. 3) proteins were not modified in a way that alters the *pI*. It could thus be
479 postulated that at least some of the TAXI- and XIP-type XIs are phosphorylated
480 whereas TLXI-type inhibitors are not.

481 For this purpose, prior to 2-DE, purified TAXI- and XIP-/TLXI-type XIs were treated
482 with λ PPase, which acts on all currently known phosphorylated amino acid residues.
483 The dephosphorylated protein patterns for TAXI-, as well as XIP- and TLXI-type XIs
484 (results not shown), were identical to the ones obtained before. This result was
485 confirmed by comparison of dephosphorylated and intact XIs with phosphorylated
486 (casein and ovalbumin) and non-phosphorylated (BSA) control proteins using 1D-
487 SDS-PAGE and Pro-Q-Diamond phosphostaining (Fig. 7A), followed by silver
488 staining (Fig. 7B). From these experiments, we can conclude that phosphorylation
489 does not contribute to the complexity of the XI spot patterns, in particular to
490 differences in *pI*. Modifications such as acetylation, methylation, deamidation and
491 sialylation all may give rise to cathodic shifts in 2-DE. Examination of these options
492 will require more extensive biochemical analyses.

493

494 **3.4.3 Micro-heterogeneity at the C-or N-terminal end of the amino acid chain**

495 Terminal truncation was investigated by including systematically N- or C-terminally
496 shortened TAXI and XIP sequence variants in the Sequest database. This way,
497 deletions of 1 or 2 amino acids at the TAXI N-terminus were frequently observed by
498 ESI-MS/MS (Supplementary Table 2). In contrast, C-terminal peptides, if observed,
499 were untruncated.

500 To further verify whether the different XI-forms are processed *in planta*, CNBr-
501 fragments from multiple spots were generated and analyzed by MALDI-MS and
502 MS/MS analysis [34]. As an example, MS analysis of the CNBr-fractions in spot 2
503 (Fig. 2A) reveals three peptides with respective m/z values of 1574.85, 1849.08 and
504 2160.22 Da. The first two correspond to internal CNBr-fragments of the TAXI-
505 725ACCN isoform (both with a homoserinelactone derivative, $\Delta m = -48$ Da) while
506 the mass of the fragment at m/z 2160.22 is in full agreement with the theoretical mass
507 of the C-terminal fragment Glu364-Leu382 (calculated molecular mass 2159.14 Da).
508 In spot 3 (Fig. 2A), three CNBr-fragments at m/z values of 1791.05, 2254.37 and
509 2160.21 Da were also observed. The two former represent internal fragments
510 indicative for TAXI-Ia (Fig. 4), while the latter coincides with the intact C-terminus.
511 The C-termini of some TAXI proteins were also identified by *de novo* sequence
512 analysis of chemically derivatized tryptic peptides. As an example, in spot 1 and 2,
513 both identified as TAXI-725ACCN, the C-terminal tryptic peptide,
514 LGFSRLPHFTGCGGL (Leu368-Leu382) (Fig. 4) was seen by MS/MS analysis.
515 CNBr-fragments were also derived for a number of the XIP-type proteins before and
516 after deglycosylation, since MS often fails to detect glycosylated peptides. In spots 34
517 and 44 (Fig. 3A), two main signals at m/z 2793.3 and 3037.4 Da were observed after
518 CNBr-cleavage. These two fragments correspond to the C- and N-terminal fragments
519 of the XIP-I-isoform, as deduced from MS/MS analysis and partial N-terminal
520 sequence analysis, respectively (results not shown). After deglycosylation, the same
521 m/z values of the XIP-I-isoform were observed in spots 2-4 (Fig. 5B), with an
522 additional fragment at 1264.6 Da. MS/MS analysis of the latter indicated that it
523 contains the N-terminal sequence, probably generated by a non-specific cleavage.
524 This N-terminal fragment was also present in spot 1 (Fig. 5B) with a satellite peak at

525 m/z 1344.5 (ΔM 80 Da). Together, this illustrates that neither C- nor N-terminal
526 processing is responsible for the different horizontal position of the XI spots which
527 share an identical MS identification.

528 **CONCLUDING REMARKS**

529 In the present study, 2-DE and subsequent tandem MS analysis were successfully
530 used to reveal the presence of complex polymorphic XI families in wheat grain and,
531 in addition, to gain insight in the genetic variability present. Moreover, this is the first
532 paper with a simultaneous emphasis on the three XI classes, currently found in wheat.
533 Thanks to a refined pre-fractionation step and the availability of improved basic pH-
534 gradient protocols, it was possible to effectively focus on a small, but from a plant
535 physiological and a wheat processing point of view, very interesting part of the wheat
536 grain proteome.

537 Although multiple XI genes were already available in public databases, we were able
538 to show that not all of them are actually expressed in wheat grains, or at least not to
539 the same extent. For instance, no variant specific tryptic peptides of TAXI-III/Ib or
540 XIP-R1/R2 were found, while the putative TAXI-725ACCN and XIP-III variants, for
541 which it was not yet known whether expression actually occurred in the mature wheat
542 caryopsis, could be identified in several (major) spots. This underlines the need for
543 integration of data on genomic and proteomic levels. The proteomic approach also
544 enabled us to investigate some ubiquitous PTMs. Glycosylation is responsible for the
545 variation in molecular mass, observed for XIP- and TLXI-type proteins. Some genetic
546 variants of TAXI- and XIP-type proteins display differences in *pI*, which could not be
547 attributed to phosphorylation or processed C- or N-termini. The existence of yet
548 unknown wheat XI gene sequences can not be excluded.

549 When looking down the road, the obtained results, including the 2-DE fingerprints of
550 TAXI-, XIP-, and TLXI-type proteins, will be instrumental in exploring the temporal
551 and spatial distribution of XIs in wheat grains by analyzing successive developmental/
552 germination stages and different milling fractions or kernel tissues, respectively.

553 Additionally, 2-DE analysis of wheat, infected with ubiquitous cereal pathogens, e.g.
554 *F. graminearum*, can provide useful information on the physiological role of TAXI-,
555 XIP-, and TLXI-type (iso)forms in plant defence. More research on such proteins,
556 important for plant resistance, can pave the way for the development of efficient
557 strategies in environment-sound plant protection.

558 In conclusion, next to providing insight in the variability of polymorphic XI families,
559 this work contributes to a better understanding of the link between XI proteins and XI
560 genes, effectively expressed in wheat. It further provides a strong basis for the
561 analysis of the temporal and spatial distribution of XIs in wheat and of the presumed
562 physiological role of TAXI-, XIP-, and TLXI-type (iso)forms in plant defence.

563 **ACKNOWLEDGEMENTS**

564 *The authors acknowledge the 'Instituut voor de aanmoediging van Innovatie door*
565 *Wetenschap en Technologie in Vlaanderen' (I.W.T., Brussels, Belgium) for their*
566 *financial support. Kurt Gebruers and Bart Samyn are postdoctoral fellows of the*
567 *Fund for Scientific Research-Flanders (F.W.O., Flanders, Belgium). The authors*
568 *would like to thank Gert Raedschelders for providing access to additional, putative XI*
569 *gene sequences and critical reading.*

570 **REFERENCES**

- 571 [1] Biely, P., Vrsanska, M., Kucar, S., in: Visser, J., Beldman, G., Kusters-van
572 Someren, M. A., Voragen, A. G. J. (Eds.), *Xylans and xylanases*, Elsevier Science
573 Publishers, Amsterdam 1992, pp. 81-94.
- 574 [2] Henrissat, B., A Classification of Glycosyl Hydrolases Based on Amino-Acid-
575 Sequence Similarities, *Biochem. J.* 1991, 280, 309-316.
- 576 [3] Simpson, D. J., Fincher, G. B., Huang, A. H. C., Cameron-Mills, V., Structure and
577 function of cereal and related higher plant (1 -> 4)-beta-xylan endohydrolases, *J.*
578 *Cereal Sci.* 2003, 37, 111-127.
- 579 [4] Giesbert, S., Lepping, H. B., Tenberge, K. B., Tudzynski, P., The xylanolytic
580 system of *Claviceps purpurea*: Cytological evidence for secretion of xylanases in
581 infected rye tissue and molecular characterization of two xylanase genes,
582 *Phytopathology* 1998, 88, 1020-1030.
- 583 [5] Kang, Z., Buchenauer, H., Ultrastructural and cytochemical studies on cellulose,
584 xylan and pectin degradation in wheat spikes infected by *Fusarium culmorum*, *J.*
585 *Phytopath.* 2000, 148, 263-275.
- 586 [6] Wanjiru, W. M., Kang, Z. S., Buchenauer, H., Importance of cell wall degrading
587 enzymes produced by *Fusarium graminearum* during infection of wheat heads, *Eur. J.*
588 *Plant Pathol.* 2002, 108, 803-810.
- 589 [7] Brito, N., Espino, J. J., Gonzalez, C., The endo-beta-1,4-xylanase xyn11A is
590 required for virulence in *Botrytis cinerea*, *Mol. Plant-Microbe Interact.* 2006, 19, 25-
591 32.
- 592 [8] Christov, L. P., Szakacs, G., Balakrishnan, H., Production, partial characterization
593 and use of fungal cellulase-free xylanases in pulp bleaching, *Process Biochem.* 1999,
594 34, 511-517.

595 [9] Courtin, C. M., Delcour, J. A., Arabinoxylans and endoxylanases in wheat flour
596 bread-making, *J. Cereal Sci.* 2002, 35, 225-243.

597 [10] Christophersen, C., Andersen, E., Jakobsen, T. S., Wagner, P., Xylanases in
598 wheat separation, *Starch-Starke* 1997, 49, 5-12.

599 [11] Debyser, W., Derdelinckx, G., Delcour, J. A., Arabinoxylan and arabinoxylan
600 hydrolysing activities in barley malts and worts derived from them, *J. Cereal Sci.*
601 1997, 26, 67-74.

602 [12] Bedford, M. R., Schulze, H., Exogenous enzymes for pigs and poultry, *Nutr. Res.*
603 *Rev.* 1998, 11, 91-114.

604 [13] Chivasa, S., Simon, W. J., Yu, X. L., Yalpani, N., Slabas, A. R., Pathogen
605 elicitor-induced changes in the maize extracellular matrix proteome, *Proteomics*
606 2005, 5, 4894-4904.

607 [14] Di, C. X., Zhang, M. X., Xu, S. J., Cheng, T., An, L. Z., Role of
608 polygalacturonase-inhibiting protein in plant defense, *Crit. Rev. Microbiol.* 2006, 32,
609 91-100.

610 [15] Debyser, W., Derdelinckx, G., Delcour, J. A., Arabinoxylan solubilization and
611 inhibition of the barley malt xylanolytic system by wheat during mashing with wheat
612 wholemeal adjunct: Evidence for a new class of enzyme inhibitors in wheat, *J. Am.*
613 *Soc. Brew. Chem.* 1997, 55, 153-156.

614 [16] McLauchlan, W. R., Garcia-Conesa, M. T., Williamson, G., Roza, M., *et al.*, A
615 novel class of protein from wheat which inhibits xylanases, *Biochem. J.* 1999, 338,
616 441-446.

617 [17] Fierens, E., Rombouts, S., Gebruers, K., Goesaert, H., *et al.*, TLXI, a novel type
618 of xylanase inhibitor from wheat (*Triticum aestivum*) belonging to the thaumatin
619 family, *Biochem. J.* 2007, 403, 583-591.

620 [18] Igawa, T., Ochiai-Fukuda, T., Takahashi-Ando, N., Ohsato, S., *et al.*, New
621 TAXI-type xylanase inhibitor genes are inducible by pathogens and wounding in
622 hexaploid wheat, *Plant Cell Physiol.* 2004, *45*, 1347-1360.

623 [19] Igawa, T., Tokai, T., Kudo, T., Yamaguchi, I., Kimura, M., A wheat xylanase
624 inhibitor gene, Xip-I, but not Taxi-I, is significantly induced by biotic and abiotic
625 signals that trigger plant defense, *Biosci. Biotechnol. Biochem.* 2005, *69*, 1058-1063.

626 [20] Gebruers, K., Debyser, W., Goesaert, H., Proost, P., *et al.*, Triticum aestivum L.
627 endoxylanase inhibitor (TAXI) consists of two inhibitors, TAXI I and TAXI II, with
628 different specificities, *Biochem. J.* 2001, *353*, 239-244.

629 [21] Fierens, K., Brijs, K., Courtin, C. M., Gebruers, K., *et al.*, Molecular
630 identification of wheat endoxylanase inhibitor TAXI-I-1, member of a new class of
631 plant proteins, *FEBS Lett.* 2003, *540*, 259-263.

632 [22] Raedschelders, G., Fierens, K., Sansen, S., Rombouts, S., *et al.*, Molecular
633 identification of wheat endoxylanase inhibitor TAXI-II and the determinants of its
634 inhibition specificity, *Biochem. Biophys. Res. Commun.* 2005, *335*, 512-522.

635 [23] Elliott, G. O., Hughes, R. K., Juge, N., Kroon, P. A., Williamson, G., Functional
636 identification of the cDNA coding for a wheat endo-1,4-beta-D-xylanase inhibitor,
637 *FEBS Lett.* 2002, *519*, 66-70.

638 [24] Stotz, H. U., Bishop, J. G., Bergmann, C. W., Koch, M., *et al.*, Identification of
639 target amino acids that affect interactions of fungal polygalacturonases and their plant
640 inhibitors, *Physiol. Mol. Plant Pathol.* 2000, *56*, 117-130.

641 [25] Trogh, I., Sorensen, J. F., Courtin, C. M., Delcour, J. A., Impact of inhibition
642 sensitivity on endoxylanase functionality in wheat flour breadmaking, *J. Agric. Food*
643 *Chem.* 2004, *52*, 4296-4302.

644 [26] Frederix, S. A., Courtin, C. M., Delcour, J. A., Substrate selectivity and inhibitor
645 sensitivity affect xylanase functionality in wheat flour gluten-starch separation, *J.*
646 *Cereal Sci.* 2004, *40*, 41-49.

647 [27] Courtin, C. M., Gys, W., Gebruers, K., Delcour, J. A., Evidence for the
648 involvement of arabinoxylan and xylanases in refrigerated dough syruing, *J. Agric.*
649 *Food Chem.* 2005, *53*, 7623-7629.

650 [28] Juge, N., Svensson, B., Proteinaceous inhibitors of carbohydrate-active enzymes
651 in cereals: implication in agriculture, cereal processing and nutrition, *J. Sci. Food*
652 *Agric.* 2006, *86*, 1573-1586.

653 [29] Sørensen, J. F., Sibbesen, O., Mapping of residues involved in the interaction
654 between the *Bacillus subtilis* xylanase A and proteinaceous wheat xylanase inhibitors,
655 *Prot. Eng. Des. Sel.* 2006, *19*, 205-210.

656 [30] Bourgois, T. M., Nguyen, D. V., Sansen, S., Rombouts, S., *et al.*, Targeted
657 molecular engineering of a family 11 endoxylanase to decrease its sensitivity towards
658 *Triticum aestivum* endoxylanase inhibitor types, *J. Biotechnol.* 2007, *130*, 95-105.

659 [31] Sørensen, J. F., Kragh, K. M., Sibbesen, O., Delcour, J. A., *et al.*, Potential role
660 of glycosidase inhibitors in industrial biotechnological applications, *Biochim.*
661 *Biophys. Acta* 2004, *1696*, 275-287.

662 [32] Gebruers, K., Brijs, K., Courtin, C. M., Goesaert, H., *et al.*, Affinity
663 chromatography with immobilised endoxylanases separates TAXI- and XIP-type
664 endoxylanase inhibitors from wheat (*Triticum aestivum* L.), *J. Cereal Sci.* 2002, *36*,
665 367-375.

666 [33] Bradford, M. M., A rapid and sensitive method for the quantitation of microgram
667 quantities of protein utilizing the principle of protein-dye binding, *Anal. Biochem.*
668 1976, *72*, 248-254.

669 [34] Laemmli, U. K., Cleavage of structural proteins during the assembly of the head
670 of bacteriophage T4, *Nature* 1970, 227, 680-685.

671 [35] Candiano, G., Bruschi, M., Musante, L., Santucci, L., *et al.*, Blue silver: A very
672 sensitive colloidal Coomassie G-250 staining for proteome analysis, *Electrophoresis*
673 2004, 25, 1327-1333.

674 [36] Blum, H., Beier, H., Gross, H. J., Improved silver staining of plant-proteins,
675 RNA and DNA in polyacrylamide gels, *Electrophoresis* 1987, 8, 93-99.

676 [37] Shevchenko, A., Tomas, H., Havlis, J., Olsen, J. V., Mann, M., In-gel digestion
677 for mass spectrometric characterization of proteins and proteomes, *Nat. Protoc.* 2006,
678 1, 2856-2860.

679 [38] Dumont, D., Noben, J. P., Raus, J., Stinissen, P., Robben, J., Proteomic analysis
680 of cerebrospinal fluid from multiple sclerosis patients, *Proteomics* 2004, 4, 2117-
681 2124.

682 [39] Martens, L., Vandekerckhove, J., Gevaert, K., DBToolkit: processing protein
683 databases for peptide-centric proteomics, *Bioinformatics* 2005, 21, 3584-3585.

684 [40] Samyn, B., Sergeant, K., Castanheira, P., Faro, C., Van Beeumen, J., A new
685 method for C-terminal sequence analysis in the proteomic era, *Nat. Meth.* 2005, 2,
686 193-200.

687 [41] Sergeant, K., Samyn, B., Debyser, G., Van Beeumen, J., De novo sequence
688 analysis of N-terminal sulfonated peptides after in-gel guanidination, *Proteomics*
689 2005, 5, 2369-2380.

690 [42] Samyn, B., Sergeant, K., Van Beeumen, J., A method for C-terminal sequence
691 analysis in the proteomic era (proteins cleaved with cyanogen bromide), *Nat. Protoc.*
692 2006, 1, 318-323.

693 [43] Beaugrand, J., Gebruers, K., Ververken, C., Fierens, E., *et al.*, Antibodies against
694 wheat xylanase inhibitors as tools for the selective identification of their homologues
695 in other cereals, *J. Cereal Sci.* 2006, *44*, 59-67.

696 [44] Dornez, E., Joye, I. J., Gebruers, K., Delcour, J. A., Courtin, C. M., Wheat-
697 kernel-associated endoxylanases consist of a majority of microbial and a minority of
698 wheat endogenous endoxylanases, *J. Agric. Food Chem.* 2006, *54*, 4028-4034.

699 [45] Edge, A. S. B., Deglycosylation of glycoproteins with trifluoromethanesulphonic
700 acid: elucidation of molecular structure and function, *Biochem. J.* 2003, *376*, 339-350.

701 [46] Goesaert, H., Elliott, G., Kroon, P. A., Gebruers, K., *et al.*, Occurrence of
702 proteinaceous endoxylanase inhibitors in cereals, *Biochim. Biophys. Acta* 2004, *1696*,
703 193-202.

704 [47] Takahashi-Ando, N., Inaba, M., Ohsato, S., Igawa, T., *et al.*, Identification of
705 multiple highly similar XIP-type xylanase inhibitor genes in hexaploid wheat,
706 *Biochem. Biophys. Res. Commun.* 2007, *360*, 880-884.

707 [48] Sansen, S., De Ranter, C. J., Gebruers, K., Brijs, K., *et al.*, Structural basis for
708 inhibition of *Aspergillus niger* xylanase by *Triticum aestivum* xylanase inhibitor-I, *J.*
709 *Biol. Chem.* 2004, *279*, 36022-36028.

710 [49] Payan, F., Flatman, R., Porciero, S., Williamson, G., *et al.*, Structural analysis of
711 xylanase inhibitor protein I (XIP-I), a proteinaceous xylanase inhibitor from wheat
712 (*Triticum aestivum*, var. Soisson), *Biochem. J.* 2003, *372*, 399-405.

713 [50] Shah, M. M., Fujiyama, K., Flynn, C. R., Joshi, L., Sialylated endogenous
714 glycoconjugates in plant cells, *Nat. Biotechnol.* 2003, *21*, 1470-1471.

715 [51] Kleinert, P., Kuster, T., Arnold, D., Jaeken, J., *et al.*, Effect of glycosylation on
716 the protein pattern in 2-D-gel electrophoresis, *Proteomics* 2007, *7*, 15-22.

717 [52] Horvath, E., Edwards, A. M., Bell, J. C., Braun, P. E., Chemical Deglycosylation
718 on a Micro-Scale of Membrane-Glycoproteins with Retention of Phosphoryl-Protein
719 Linkages, *J. Neurosci. Res.* 1989, 24, 398-401.

720 **FIGURE CAPTIONS**

721 **Figure 1.** Silver stained 2-DE pattern (pH 6-11; 15% PAA gel) of low salt
722 extractable wheat seed proteins (cultivar Claire, 350 µg). Rectangles represent
723 particular regions containing the three types of XIs, visualised by western blotting and
724 probing of membranes with specific anti-TAXI, anti-XIP or anti-TLXI PABs.

725

726 **Figure 2.** Colloidal CBB stained 2-DE patterns (pH 6-11; 15% PAA gels) of TAXI-
727 type XIs (40 µg) purified from the wheat cultivars Claire (A), Koch (B) and Zohra
728 (C). Numbered spots (A) were excised and analysed by LC-ESI-MS/MS (Table 1 and
729 Supplementary Table 1).

730

731 **Figure 3.** Colloidal CBB stained 2-DE patterns (pH 6-11; 15% PAA gels) of XIP-
732 and TLXI-type XIs (40 µg) purified from the wheat cultivars Claire (A), Koch (B)
733 and Zohra (C). Numbered spots (A) were excised and analysed by LC-ESI-MS/MS
734 (Table 1 and Supplementary Table 1).

735

736 **Figure 4.** Amino acid sequence alignment of TAXI-type XIs, without signal
737 sequence (Clustal W, EBI, default parameters). (✓) indicates the conserved cleavage
738 site separating the 30 and 10 kDa TAXI polypeptides. Underlined amino acids are
739 LC-ESI-MS/MS sequenced peptide fragments (in agreement with Supplementary
740 Table 2). CNBr-fragments are indicated in italics.

741

742 **Figure 5.** Colloidal CBB stained 2-DE patterns (pH 6-11; 15% PAA gels) of
743 chemically deglycosylated TAXI-type (A) and XIP-/TLXI-type XIs (B) (cultivar
744 Claire, 40 µg). Arrows indicate the shift in pI after deglycosylation, compared to the

745 original 2-DE patterns (Figs. 2A and 3A). Numbered spots (1-4) were submitted to C-
746 terminal analysis.

747

748 **Figure 6.** 2-DE patterns (pH 6-11; 15% PAA gels) after staining with the fluorescent
749 Pro-Q Emerald 300 glycoprotein gel stain, showing glycosylated proteins in TAXI-
750 type (A) and XIP-type XIs (B) of wheat cultivar Claire (40 µg).

751

752 **Figure 7.** SDS-PAGE profile (under reducing conditions) of XI proteins, stained with
753 Pro-Q Diamond phosphoprotein gel stain (A) and subsequently, using the sensitive
754 silver staining (B) procedure. Casein and ovalbumin were used as positive control
755 samples, while BSA was applied as a negative control. TAXI-type XIs (0.4 µg, 1);
756 XIP/TLXI-type XIs (1.0 µg, 2); TLXI-type XIs (0.4 µg, 3); casein (0,4 µg, 4);
757 ovalbumin (0,4 µg, 5); BSA (0,4 µg, 6).

Table 1. Tandem MS identification of spots, excised from 2-DE gels (pH 6-11; 15% PAA gels) of affinity-purified proteins originating from whole meal of wheat cultivar Claire.

Spot ID ^a	GenBank ID	Species	Protein Name	Theor. MW	Theor. pI
TAXI-type xylanase inhibitors (40 kDa polypeptides)^b					
1-2	EU082811	<i>Triticum aestivum</i>	TAXI-725ACCN	39.1	7.6
3,5	AJ438880	<i>Triticum aestivum</i>	TAXI-Ia	38.8	8.2
4,6-8	AB114628	<i>Triticum aestivum</i>	TAXI-IV	39.7	8.6
9-10	AJ697849	<i>Triticum aestivum</i>	TAXI-IIa	40.3	8.4
11-13	AB114628/AJ697850	<i>Triticum aestivum</i>	TAXI-IV/TAXI-IIb	39.7/40.3	8.6/8.4
TAXI-type xylanase inhibitors (30 kDa polypeptides)^b					
14-19,23-24	EU082811	<i>Triticum aestivum</i>	TAXI-725ACCN	27.0	8.6
20-21	AJ438880	<i>Triticum aestivum</i>	TAXI-Ia	26.9	8.7
22	AB114628	<i>Triticum aestivum</i>	TAXI-IV	27.0	9.0
XIP-type xylanase inhibitors^c					
25-29,31	AB204556	<i>Triticum aestivum</i>	XIP-III	30.5	6.9
30, 32-51	Q8L5C6	<i>Triticum aestivum</i>	XIP-I	30.3	8.3
TLXI-type xylanase inhibitors^d					
52-55	AJ786601	<i>Triticum aestivum</i>	TLXI	15.6	8.4
α-amylase inhibitors^d					
56-57	CAA35597	<i>Triticum aestivum</i>	α -amylase inhibitor CM3	18.2	7.4
58	AAV39518	<i>Triticum aestivum</i>	0.19 dimeric α -amylase inhibitor	13.3	6.7
59	CAA35598	<i>Triticum aestivum</i>	α -amylase inhibitor CM1	15.5	7.5
60	AAV39519	<i>Triticum aestivum</i>	0.19 dimeric α -amylase inhibitor	13.2	6.5
61	CAA39099	<i>Triticum turgidum</i>	α -amylase inhibitor CM2	15.5	6.9

a) Spot ID as indicated in Figs. 2A and 3A.

b) TAXI variants, tentatively assigned by manually calculating the maximal number of significantly scored, variant matching peptide hits in each spot (see Supplementary Table 2).

c) XIP variants, tentatively assigned by manually calculating the maximal number of significantly scored, variant matching peptide hits in each spot (see Supplementary Table 3).

d) Significantly scored peptides and Sequest/Mascot hits listed in Supplementary Table 1. Sequest cross correlation score ≥ 3.5 for triply charged peptide ions; Sequest cross correlation score ≥ 2.5 for doubly charged peptide ions; Sequest cross correlation score ≥ 1.8 for singly charged peptide ions; Mascot Expect value ≤ 0.05 .

Figure 1.

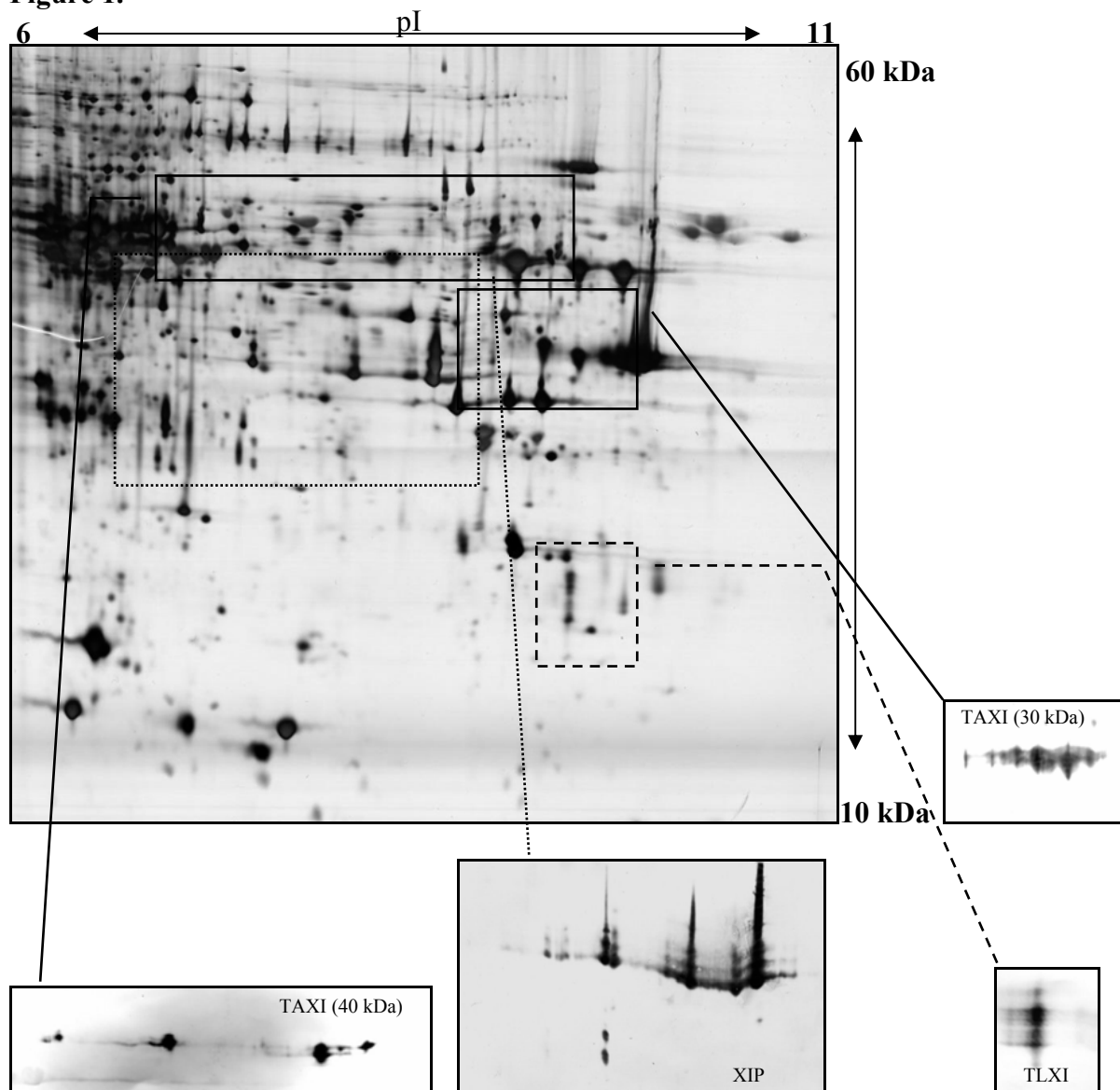


Figure 2.

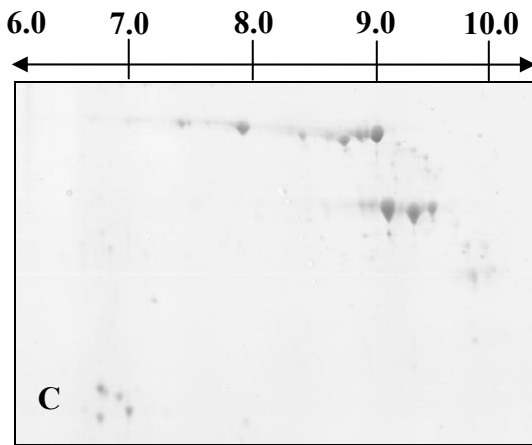
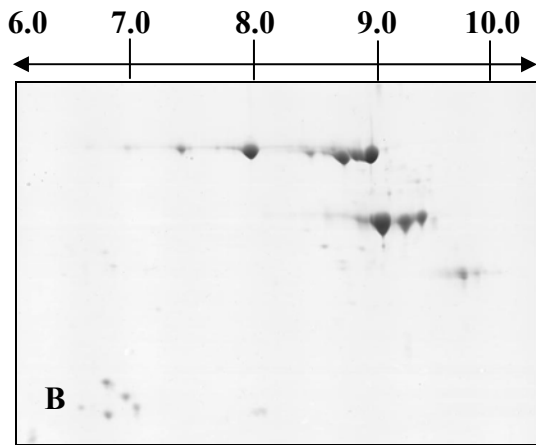
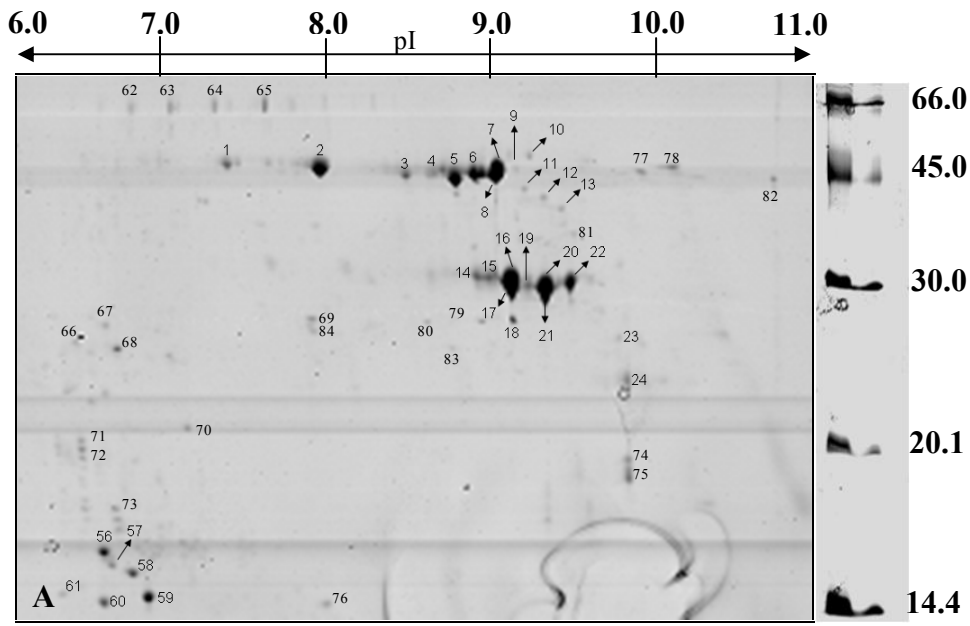


Figure 3

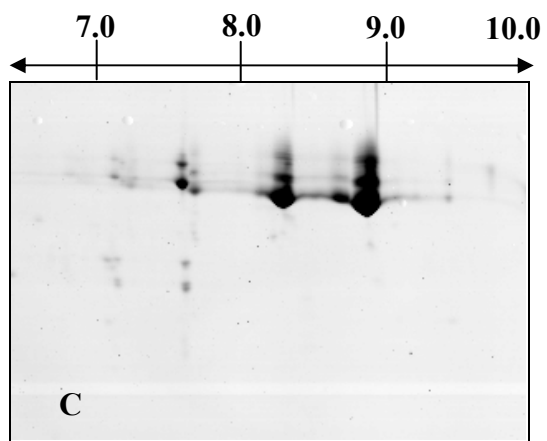
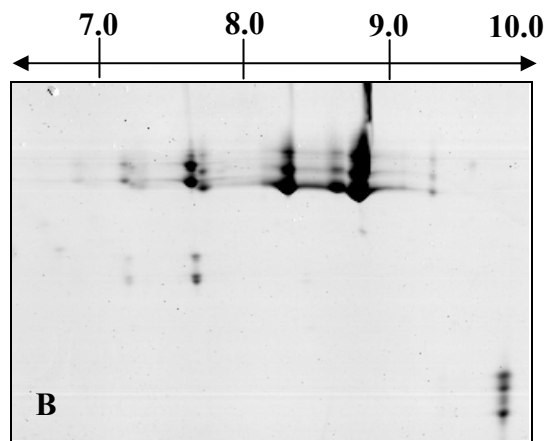
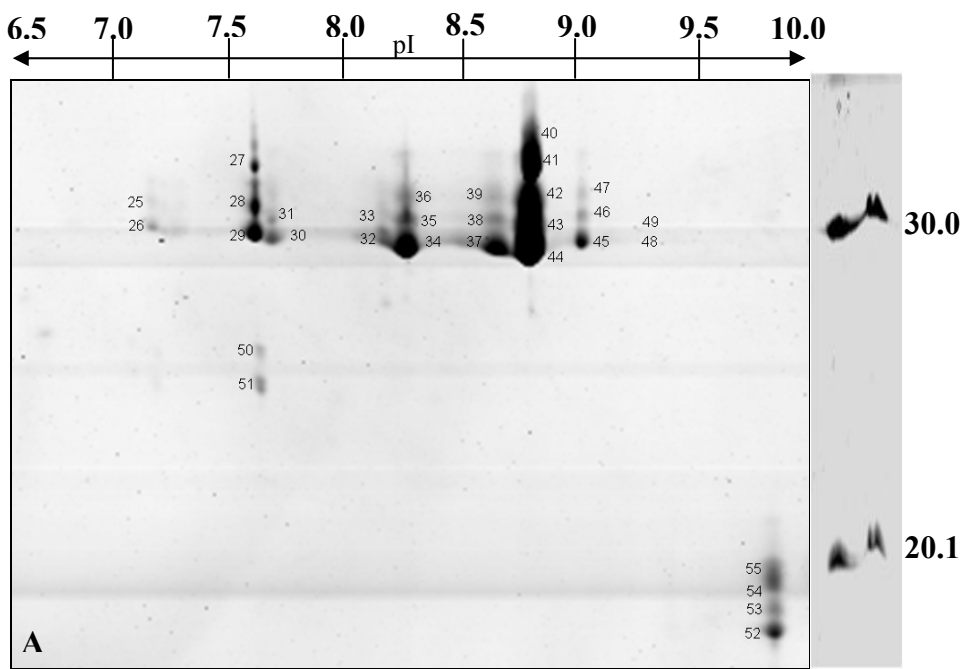


Figure 4.

TAXI-IIb EGLPVLAPVTKDTATSLYTIPFDGANLVLDVAGPLVWSTCDGGQPPAEIPCSSPTCLLA 60

TAXI-IV KGLPVLAPVTKDTATSLYTIPFDGANLVLDVAGPLVWSTCDGGQPPAEIPCSSPTCLLA 59

TAXI-Ib/III KGLPVLAPVTKDTATSLYTIPFDGASLVLDVAGPLVWSTCEGSQPPAEIPCSSPTCLLS 60

TAXI-IIa KGLPVLAPVTKDTATSLYTIPFDGASLVLDVAGLLVWSTCEGGQSPAIEIACSSPTCLLA 60

TAXI-725ACCN --LPVLAPVTKDPATSLYTIPFDGASLVLDVAGPLVWSTCEGGQPPAEIPCSSPTCLLA 58

TAXI-725ACC KGLPVLAPVTKDTATSLYTIPFDGASLVLDVAGPLVWSTCDGGQPPAEIPCSSPTCLLA 60

TAXI-Ia --LPVLAPVTKDPATSLYTIPFDGASLVLDVAGPLVWSTCDGGQPPAEIPCSSPTCLLA 58

*****.*****.***** *****:*.*.****.*****:

TAXI-IIb NAYPAPGCPAPSCGSDRHDKPCTAYPYNPVTGACAAGSLFHTKFVANTTDGNKPVSKVNV 120

TAXI-IV NAYPAPGCPAPSCGSDRHDKPCTAYPYNPVTGACAAGSLFHTKFVANTTDGNKPVSKVNV 118

TAXI-Ib/III NAYPAPGCPAPSCGSDRHDKPCTAYPSNPVTGACAAGSLFHTKFAANTTDGNKPVSEVNV 120

TAXI-IIa NAYPAPGCPAPSCGSDRHDKPCTAYPSNPVTGACAAGSLFHTRFAANTTDGNKPVSEVNV 120

TAXI-725ACCN NAYPAPGCPAPSCGSDTHDKPCTAYPYNPVTGACAAGSLFHTRFAANTTDGSKPVSKVNV 118

TAXI-725ACC NAYPAPGCPAPSCGSDKHDKPCTAYPYNPVTGACAAGSLFHTRFAANTTDGSKPVSKVNV 120

TAXI-Ia NAYPAPGCPAPSCGSDKHDKPCTAYPYNPVSAGACAAGSLSHTRFVANTTDGSKPVSKVNV 118

***** ***** * ***:***** **:*.*****.*****:***

TAXI-IIb GVVAACAPSKLLASLPRGSTGVAGLADSGGLALPAQVASAQKVANRFLLCCLPTGGGLGVAIF 180

TAXI-IV GVVAACAPSKLLASLPRGSTGVAGLADSGGLALPAQVASAQKVANRFLLCCLPTGGGLGVAIF 178

TAXI-Ib/III GVLAACAPSKLLASLPRGSTGVAGLANSGLALPAQVASTQKVANRFLLCCLPTGGGLGVAIF 180

TAXI-IIa RVLAACAPSKLLASLPRGSTGVAGLAGSGLALPSQVASAQKVANKFLLCCLPTGGPGVAIF 180

TAXI-725ACCN GVLAACAPSKLLASLPRGSTGVAGLADSGGLALPAQVASAQKVAKRFLLCCLPTGGPGVAIF 178

TAXI-725ACC GVLAACAPSKLLASLPRGSTGVAGLADSGGLALPAQVASAQKVANRFLLCCLPTGGPGVAIF 180

TAXI-Ia GVLAACAPSKLLASLPRGSTGVAGLANSGLALPAQVASAQKVANRFLLCCLPTGGPGVAIF 178

*:***.*****.*****.*****:****:****:;***** *****

TAXI-IIb GGGPLPWPQFTQSMDYTPLVAKGGSPAHIYISLKSIVKVENTRVPVSERALATGGVMLSTRL 240

TAXI-IV GGGPLPWPQFTQSMDYTPLVAKGGSPAHIYISLKSIVKVENTRVPVSERALATGGVMLSTRL 237

TAXI-Ib/III GGGPLPWPQFTQSMDYTPLVAKGGSPAHIYISLKSIVKVENTRVPVSERALATGGVMLSTRL 240

TAXI-IIa GGGPLPWPQFTQSMDYTPLVAKGGSPAHIYSARSIVKVENTRVPVSERALATGGVMLSTRL 240

TAXI-725ACCN GGGPLPWPQFTQSMPTPLVTKGGSPAHIYSARFIEVGDTRVPVSEGALATGGVMLSTRL 238

TAXI-725ACC GGGPVWPWPQFTQSMPTPLVTKGGSPAHIYSARFIEVGDTRVPVSEGALATGGVMLSTRL 240

TAXI-Ia GGGPVWPWPQFTQSMPTPLVTKGGSPAHIYSARSIVVGDTRVPVPEGALATGGVMLSTRL 238

****:***** *****:***** : * * :****:.* *****

TAXI-IIb PYVLLRRDVYRPFVDAFTKALAAQPAN[^]GAPVARAVKPVAPFELCYDTKSLGNNLGGYWVP 300

TAXI-IV PYVLLRRDVYRPFVDAFTKALAAQPAN[^]GAPVARAVKPVAPFELCYDTKSLGNNLGGYWVP 297

TAXI-Ib/III PYVLLRRDVYRPFVGAFTKALAAQPAN[^]GAPVARAVKPVAPFELCYDTKSLGNNLGGYWVP 300

TAXI-IIa PYVLLRRDVYRPLVDAFTKALAAQPAN[^]GAPVARAVKPVAPFELCYDTKTLGNNPGGYWVP 300

TAXI-725ACCN PYAVLRRDVYRPLVDAFTKALAAQHAN[^]GAPVARAVEPVAPFGVCYDTKTLGNNLGGYSVP 298

TAXI-725ACC PYAVLRRDVYRPLVDAFTKALAAQHAN[^]GAPVARAAEPVAPFGVCYDTKTLGNNLGGYSVP 300

TAXI-Ia PYVLLRPDVYRPLMDAFTKALAAQHAN[^]GAPVARAVEAVAPFGVCYDTKTLGNNLGGYAVP 298

.: *****:;***** *****.: ***** :*****:**** ** **

TAXI-IIb NVGLAVDGGSD-WAMTGKNSMVDVKPGTACVAFVEMKGVEAGDGRAPAVILGGAQMEDFV 359
TAXI-IV NVGLAVDGGSD-WAMTGKNSMVDVKPGTACVAFVEMKGVEAGDGRAPAVILGGAQMEDFV 356
TAXI-Ib/III NVGLAVDGGSD-WAMTGKNSMVDVKPGTACVAFVEMKGVEAGDGRAPAVILGGAQMEDFV 359
TAXI-IIa NVLELDGGSD-WALTGKNSMVDVKPGTACVAFVEMKGV DAGDSAPAVILGGAQMEDFV 359
TAXI-725ACCN NVQLALDGGSDTWTMTGKNSMVDVKPGTACVAFVEMKGVEAGDGRAPAVILGGAQMEDFV 358
TAXI-725ACC NVQLGLDGGSDTWTMTGKNSMVDVKPGTACVAFVEMKGVEAGDGRAPAVILGGAQMEDFV 360
TAXI-Ia NVQLGLDGGSD-WTMTGKNSMVDVKQGTACVAFVEMKGVAAGDGRAPAVILGGAQMEDFV 357

:**

TAXI-IIb LDFDMEKKRLGFSRLPQFTGCSSFN FARST 389
TAXI-IV LDFDMEKKRLGFSRLPQFTGCSSFN FAGST 386
TAXI-Ib/III LDFDMEKKRLGFLRLPHFTGCGS----- 382
TAXI-IIa LDFDMEKKRLGFLRLPHFTGCSSFN FARST 389
TAXI-725ACCN LDFDMEKKRLGFSRLPHFTGCGGL----- 382
TAXI-725ACC LDFDMEKKRLGFSRLPHFTGCGGL----- 384
TAXI-Ia LDFDMEKKRLGFSRLPHFTGCGGL----- 381

*****:*****

Figure 5.

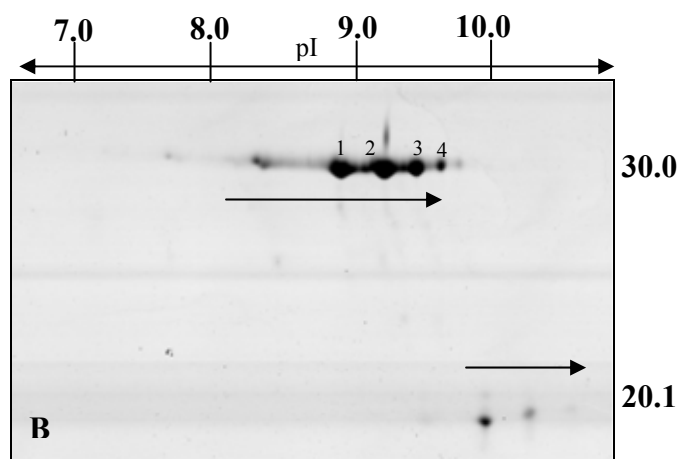
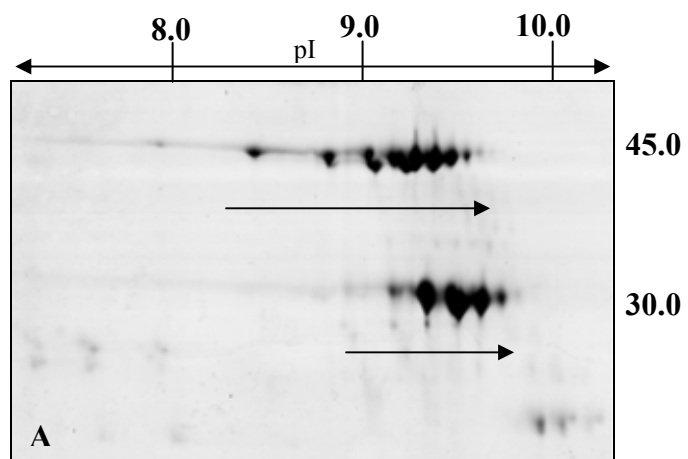


Figure 6.

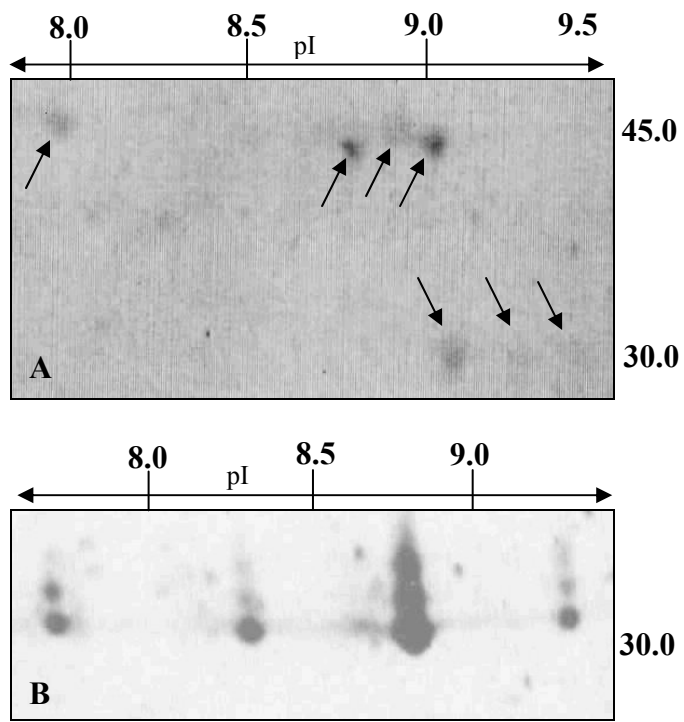


Figure 7.

